AD-A146 762 SCATTERING FROM MULTI-SCALE SURFACE(U) ROYAL SIGNALS 1/1
AND RADAR ESTABLISHMENT MALVERN (ENGLAND)
D L JORDAN ET AL. FEB 84 RSRE-MEMO-3656 DRIC-BR-92719
UNCLASSIFIED F/G 20/6 NL

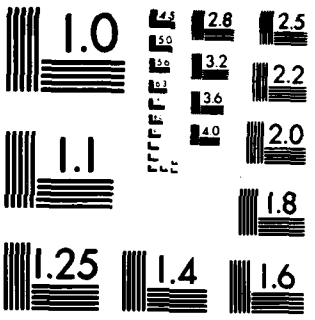

SCATTERING FROM MULTI-SCALE SURFACE

Authors: D L Jaffan, R C Shellim,
E Jakeman

PROCUREMENT EXECUTIVE,
MINISTRY OF DEFENCE,
R S R E MALVERN,
WORCS.

UNLIMITED

ROYAL SIGNALS AND RADAR ESTABLISHMENT

Memorandum 3656

TITLE: SCATTERING FROM MULTI-SCALE SURFACES

AUTHOR: D L Jordan, R C Hollins, E Jakeman

DATE: February 1984

SUMMARY

The purpose of this memorandum is to collate experimental and theoretical work on CO_2 laser scattering from multi-scale surfaces. The emphasis is on non-gaussian scattering and covers both solid and liquid surfaces. The relevance of the work to practical systems, including microwave radar, is emphasised.

RSRE MEMORANDUM NO 3656

SCATTERING FROM MULTI-SCALE SURFACES

D L Jordan, R C Hollins, E Jakeman

1. Introduction

The random pattern of bright and dark regions produced in the far-field when coherent light is scattered by a rough surface is usually referred to as 'speckle', and may be considered to be well understood [1]. By contrast, a wide variety of other related phenomena, both in the optical and the microwave region remain poorly understood [2]. These include naturally occurring optical phenomena such as the twinkling of starlight [3], the glittering of a sunlit sea surface and the caustic patterns produced on the floor of a shallow pool by sunlight playing on the rippling water surface [4]. Thus 'speckle' or gaussian scattering is a term normally reserved for the pattern generated by interference between contributions from a large number of scattering centres. Whatever their individual structure, the optical field is gaussian distributed by virtue of the central limit theorem, and all of its statistical and correlation properties are specified once its first order space-time correlation function or field spectrum has been measured. The spatial dependence of this quantity is purely determined by the projected scattering area contributing to the field at the detector. However, the natural phenomena mentioned above are obviously not gaussian interference effects as they are generated by scattering of white light (broadband radiation) and the statistical, temporal and spatial coherence properties of the scattered radiation are sensitive to the detailed internal structure of the scattering medium. The study of these and other non-gaussian scattering phenomena is also important to non-optical scattering, such as microwave (and mm wave) signal fluctuations, including high resolution microwave sea echo [5] and the fading of radio waves.

The simplest mathematical model known to generate scintillation effects is the phase changing screen, which introduces spatially random distortions into an incident planar wavefront. Amplitude fluctuations then develop during the course of free propagation beyond the scattering plane [6]. Almost all theoretical treatments of the phase-screen problem have assumed that the wavefront distortions (or equivalently the surface height fluctuations), constitute a joint-gaussian process so that only the correlation function or spectrum of the fluctuations is needed to complete the statistical model. Many authors have adopted a gaussian model for the spectrum, which corresponds physically to a smoothly varying surface containing fluctuations of roughly the same characteristic size. When the surface height variations are comparable to or exceed the wavelength of the incident radiation, this type of surface leads to amplitude fluctuations which are dominated by the presence of geometrical optics effects - caustics or singularities [7, 8]. This is referred to as a type II surface and is illustrated in Fig 1(a). When such a target is illuminated with a laser beam of variable width the contrast of the scattered intensity pattern, defined in terms of averages over the light intensity I by

$$C = \left\{ \frac{\langle I^2 \rangle}{\langle I \rangle^2} - 1 \right\}^{\frac{1}{2}} \qquad (1)$$

has the form in the far-field shown in Fig 1(b). At large spot diameters the illuminated region is much larger than the spatial correlation length of the surface height fluctuations and the contrast is unity, reflecting the noise-like or gaussian nature of light scattered by many independent scatterers. As the illuminated spot size is reduced, the central limit theorem no longer applies because of the limited number of independent scattering regions, and the contrast increases to very high values in this non-gaussian scattering region. A similar behaviour is observed in the Fresnel region, but here the independent parameter is not illuminated spot size, but distance from phase screen (spot width assumed infinite). Close to the screen there are only amplitude fluctuations; further away the contrast peaks due to caustics. Even further away the contrast relaxes to its gaussian value of unity. Jakeman and Pusey [9] have given a simple physical picture of the origin of non-gaussian fluctuations in radiation scattered from very rough surfaces using a facet model and compared it with more sophisticated treatments. Jakeman [10] has reviewed experimental and theoretical work on surface roughness measurements using non-gaussian scattering techniques and assuming single-scale smoothly-varying surfaces.

Although a wealth of experimental data on the fading of radio waves, interplanetary scintillation, acoustic reverberation etc has accumulated over the years, detailed testing of theoretical predictions had to await the results of controlled and well characterised laboratory experiments. The first of these was published in the mid-seventies by Pusey and Jakeman [11] who made measurements of the effect of illuminated spot size on the statistics of visible laser light scattered by a turbulently convecting liquid crystal. Their results were in reasonable though not complete agreement with the predictions of the smooth single-scale model. Measurements on rigid surfaces have generally given much poorer agreement [12, 13].

The probable reason for this is that most solid scatterers do not posess smooth single-scale surfaces ie they are multi-scale surfaces. Consequently predictions based on type II surfaces are gross oversimplifications. Following the work of Mandelbrot [14] one class of such scatterers have become known as 'fractals'. Unlike the smoothly varying surface, which is mathematically speaking 'continuous and differentiable to all orders', the fractal surface is 'continuous but not differentiable' and contains random structure down to arbitrarily small scales. The concept of rays is inappropriate for such models; such surfaces are called type I surfaces. The important elements of this model can be understood from fig 2 [15], which shows a step-like structure which generates only diffraction and interference effects - all the rays (normals) from the surface are parallel so no geometrical features occur in the scattered intensity pattern. This is a property shared with fractal surfaces. In addition fractal surfaces contain inhomogeneities of many sizes, the spatial spectrum of the height fluctuations being a simple power law. Unlike the smoothly-varying surface, fractal surfaces lead to very modest contrast values, the peak shown in Fig 1(b) only reaching ~ 1.5 instead of as high as 10, as commonly found for single-scale smoothly-varying surfaces.

A comparison of the predictions of various one-dimensional or 'corrugated' surface models has been given by Jakeman and McWhirter [16] who considered a truncated linear power law height correlation function. A more detailed theoretical study of corrugated power law models was made by Rumsey [17] and Berry [18] whilst numerical results for two-dimensional isotropic surfaces have been given by Marians [19] for the linear case and Furuhama [20] for the

5/3 (Kolmogorov) case. However, until the work of Jordan et al [21] there were no reported measurements of the statistics of radiation scattered by a fractal surface, in spite of its obvious relevance to optical, infra-red and microwave scattering from both natural and man-made targets.

One serious problem for Type I surface scattering is the role played by scale sizes small compared to the wavelength of the incident radiation. These may not be properly included in the usual Huygens-Fresnel approximate formulation of the *scattering* problem. Moreover, until the work of Jordan et al [21] all laboratory phase-screen experiments had been performed using visible radiation. Since mechanical profile measurements are limited to scales sizes of order 0.5 μm, accurate characterisation of surfaces with scale sizes much less than the wavelength has not been possible. In order to remedy this situation we have carried out experiments using 10.6 μm radiation from a CO_2 laser.

In this memo we first show results of gaussian speckle measurements using CO_2 radiation with both direct and heterodyne detection (of importance in CO_2 laser rangefinding). We then, after briefly reviewing the theoretical situation with regard to fractals, present measurements of the surface profiles of various scatterers and show that in general all rough solid surfaces can be regarded as fractal over some range of scale sizes. Then, using a phase screen that exhibits fractal properties over at least two decades of scale sizes, we briefly present some of the experimental measurements of the non-gaussian scattering by this target. Finally we present preliminary measurements of the surface profile of water waves and suggest that scattering from the sea surface (for example by high resolution microwave radar) may be described by a third type of surface model (Type III), called a sub-fractal

(Fig 3), which is intermediate between a Type I and a Type II surface. In this latter case the surface height is continuous and differentiable but its slope is fractal [22]. The concept of rays is valid for this model, but in the absence of higher surface derivatives no geometrical catastrophies occur in the propagating wave field.

2. Gaussian Speckle Measurements

Full details of these experiments are given in Jordan and Hollins [23]. Measurements were made of the statistics of the speckle pattern produced in transmission by a cw CO_2 laser beam scattered by a germanium phase screen. The surface-height fluctuations were approximately gaussian distributed with a standard deviation of 35 μm, which is considerably larger than the wavelength (10.6 μm). The correlation width of the height fluctuations was 600 μm.

The diameter of the illuminating beam ensured a minimum of 130 independent scatterers; hence gaussian speckle statistics were to be expected.

Fig 4 shows the first order probability-density distribution as measured using direct detection; it is the result of 500 measurements, the scatterer being moved between each one. Also shown is a theoretical negative exponential distribution curve

$$p(I)dI = \frac{1}{\langle I \rangle} \exp\left(-\frac{I}{\langle I \rangle}\right) \qquad (2)$$

having the measured value of the mean intensity $\langle I \rangle$. The measured value of the contrast was 0.98 in reasonable agreement with the expected value of unity. Fig 5 shows the measured distribution of the amplitude V of the heterodyne beat note of the scattered radiation against a local oscillator beam. Also shown is the expected Rayleigh distribution

$$p(V)dV = \frac{2V}{\langle V^2 \rangle} \exp\left(-\frac{V^2}{\langle V^2 \rangle}\right) \qquad (3)$$

Again the measured contrast of 0.51 ± 0.03 was in good agreement with the predicted value of 0.522.

The above results show that familiar speckle phenomena may be demonstrated with reasonable accuracy using 10.6 μm CO_2 radiation. The reasons for doing this were two-fold. Firstly, a full understanding of speckle phenomena is essential to our programme of work on CO_2 pulsed coherent detection (including the detection of quantum limited speckle signals), and secondly, the use of the long wavelength of CO_2 allows accurate mechanical characterisation of the scattering surface profile to $\lambda/20$; this is of great importance in our studies of non-gaussian scattering from multi-scale surfaces.

3. Surface Profile Studies

In this section we shall firstly outline our studies of the detailed characterisation of a fractal phase screen. We will then briefly mention some of our less detailed work on a wide range of other surfaces we have investigated. The spatial power spectrum p(k) of a fractal surface varies inversely as (spatial frequency) $^{\upsilon+1}$ [21] ie

$$P(k) = \frac{A}{|k|^{\upsilon+1}}$$

where υ ($0<\upsilon<2$) is related to the Hausdorff-Besicovitch dimension D of a section profile of the surface by $\upsilon = 2(2-D)$. The above form of the power spectrum indicates that a sample of finite length taken from a true fractal surface will never, however long, completely represent its properties. Real surfaces cannot therefore be treated as stationary random processes, as usually assumed. The area under the spectrum, which is the variance of the height distribution or, the square of the rms roughness, is thus most heavily influenced by the longest wavelengths in the sample ie the roughness is related to the length of sample or to the measured bandwidth. Experimental evidence of this for various surfaces is given in Sayles and Thomas [24]. Since the surface height variance $\langle h^2 \rangle$ and spatial autocorrelation function $\langle h(r)\, h(r+\delta) \rangle$ are infinite for an ideal infinite fractal the surface is defined in terms of the structure function

$$S(\delta) = \langle [h(\underline{r}) - h(\underline{r}+\delta)]^2 \rangle = L^{2-\nu}|\delta|^{\nu} \qquad (5)$$

where h is the local surface height and L is the topothesy [14, 18]. Physically, L is the distance over which the chord joining two h-values has an rms slope of one radian. In practice, a real target will exhibit an inner

scale length (either real or measurement limited) and an outer scale size [21].

A fractal phase screen has been produced [21] by mechanically roughning a piece of germanium with a small engraving tool moved randomly over its surface. Fig 6 shows surface height profiles taken along a one-dimensional scan across its surface using a 'Talysurf' stylus instrument. The probability distribution for the height difference between two points of given separation along such a scan $P[h(x) - h(x + \delta)]$ is shown in Fig 7 for δ=70 μm. A gaussian curve of the same variance as the measured distribution is also shown, indicating that the approximation of a gaussian distribution of height differences is quite realistic. The structure function $S(\delta)$ is shown in fig 8 as a log-log plot. The almost linear form of this plot indicates that $S(\delta)$ follows a power low fairly closely over two decades in δ, illustrating the self-affinity of the properties of the fractal surface over a wide range of scale sizes. The saturation of the curve at large separations shows the presence of an outer scale size beyond which the fractal properties are not displayed; the surface appears nominally planar when viewed in low resolution. The spatial power spectrum of the profile is shown in fig 9, again in log-log form.

The profile measurements shown here support the description of the phase screen as a fractal with an almost gaussian distribution of surface heights, and displaying a high degree of self-affinity over two decades in scale size. A fractal dimension of $D = 1.37 \pm 0.07$ may be determined from figs 8 and 9; this indicates that the surface is slightly smoother than a Brownian fractal ($D = 1.5$) but the analytically convenient Brownian fractal still provides useful guidelines. A topothesy of approximately 0.15 μm is also indicated.

Following the above detailed study of the germanium phase screen we carried out a limited study of the surface profiles of a wide range of solid surfaces. In each case the surface profile was measured using a 'Talysurf' stylus instrument and the structure function and power spectrum determined. Measurements of coarse sand-paper showed that it behaved as a fractal over the range 5 μm (limited below this by uncertainties in reading the Tallysurf trace) to approximately 300 μm with a fractal dimension of 1.2. Similarly perspex which had been heated and allowed to cool, thus demonstrating plastic flow, also behaved as a fractal over the range 5 μm to ~ 200 μm, this time with a fractal dimension of 1.3. Measurements were also made of several samples of GaAs grown by MOCVD. A photomicrograph of etched (111) GaAs is shown in fig 10. Again this showed fractal behaviour, the upper limit of δ being only ~ 20 μm in this case. The fractal dimension was 1.5.

Surface profile measurements were also made of brick, rough metal, woods-metal, sand-blasted metal and germanium etc, and all showed fractal behaviour with D in the range 1.2 - 1.6. This is in accord with the work of Sayles and Thomas [24] who studied the surface finish of objects ranging from motorways to the hull plate of a ship, and in all cases found they exhibited fractal behaviour over a significant range of spatial frequencies. In all they studied scale sizes from 10^{-5}m to 100m. In a physical optics approach the scale sizes affecting scattering must span the range where height fluctuations are extremely small over distances much smaller than the wavelength, to large height fluctuations over large distances. Consequently to correctly model solid surface scattering, either in the visible, the infra-red or the microwave region, it is necessary to understand fractal scattering.

To this end we have carried out measurements of the statistics of intensity scintillations of 10.6 μ m CO_2 laser radiation scattered from the germanium fractal phase screen described in detail earlier. Both direct and heterodyne measurements have been made. Fig 11 shows contrast measurements obtained in the Fresnel region, the radiation being focussed onto the germanium phase screen via a 5cm focal length lens. The relatively small contrast enhancement, which is predicted to be a characteristic of fractal scattering is immediately obvious.

The usual starting point for phase screen calculations is the Huygens-Fresnel approximate solution of Maxwells equations [16]

$$\varepsilon^{+}(\underline{R},t) = \frac{iE_o}{2\lambda R}\exp\left[i(kR-wt)\right]\int_{-\infty}^{\infty} d^2\underline{r}^1 \exp\left[ik\kappa r^{1^2} - ik\underline{r}'.\underline{r}/R + i\phi(r^1;t) - \frac{r^{1^2}}{W^2}\right] \tag{6}$$

where $\kappa = \frac{1}{2}\left(\frac{1}{\sigma}+\frac{1}{R}\right)$

This formula describes the free propagation to a point $\underline{R} \equiv (\underline{r}, z)$ of a scalar wave of complex amplitude ε^{+}, incident normally, with radius of curvature σ and gaussian amplitude profile of width W on a scatterer in the z=o plane which introduces random phase fluctuations of magnitude ϕ. Equation (6) is restricted to solutions in which small-angle scalar diffraction theory can be applied ie where the Kirchoff approximation is valid. This is however a questionable assumption for fractal scatterers because, as mentioned earlier they imply the presence of scale sizes comparable to, and smaller than, the wavelength of the incident radiation. However, in practice there will often be a high frequency cut-off in the phase fluctuation spectrum of the scatterer. Provided the scattering power of inner scale sized irregularities is small ie their rms 'height' is much smaller than a wavelength, then the basic scattering characteristics of the fractal model will be unaffected in near specular directions. Small scale roughness will however contribute significantly to large angle scattering, so that some doubt must exist as to the validity of Fraunhofer large angle scattering resluts obtained by using a fractal model for ϕ in eq (6). The actual magnitude of separations leading to 'significant' height differences in these experiments can be deduced from eqn (5) as $\delta \sim 75$ μm (this corresponds to ~ 3 scattering elements at the peak of the contrast curves of fig 11). Previous theory [16] has suggested that fractal surfaces behave as if composed of independently diffracting elements of this size if the Kirchoff approximation is valid. Since the elements are much bigger than the wavelength in the present experiments the Kirchoff approach is at least a consistent one.

It should be stressed that the question of the range of validity of the Kirchoff approximation is an important problem of current interest. It arises in the present context because the usual criterion involving local surface curvature can no longer be invoked for a surface which is not differentiable. It is reasonable to suppose that this criterion should be replaced by one based on the topothesey L, which is a measure of the rate at which the surface height changes. Thus when L is of order of the wavelength, surface elements smaller than L will be weakly scattering with rapid changes in height of only small magnitude taking place within them. It may well be that the physical optics approximation can be used if $L \ll \lambda$, a criterion satisfied in the present

experiments. However there is considerable scope for more work in this general area.

The angular dependence of the mean scattered intensity $\langle I \rangle$ in the Fraunhofer regime as determined using direct detection is shown in Fig 12. Also shown is a theoretical curve from [21]. A gaussian phase autocorrelation function, as commonly used in scattering theory would have given a straight line on this plot. The very slow fall-off of the mean scattered intensity is obvious, having fallen to only 50% of the $\theta = 0^o$ value by 30^o; this is a reflection of the importance of the small-scale structure.

The probability distribution of the scattered intensity in the Fraunhofer regime was measured by placing the detector on axis and randomly scanning the germanium scatterer transversely across the illuminating beam. The resultant normalised moments of the scattered intensity are shown in fig 13 for two values of the incident beamwidth, corresponding respectively to the non-gaussian contrast maximum and to a larger value when gaussian field statistics are expected. Also shown are the moments of a negative exponential distribution and a K-distribution; more details are given in Jordan et al [25]. It can be seen that the negative exponential intensity distribution characteristic of a gaussian field distribution closely fits the observed distribution far from the contrast peak. As the beamwidth is reduced from large values, the intensity distribution shows somewhat stronger fluctuations, the moments approaching (but not reaching) the values characteristic of a K-distribution near the contrast peak. Also shown are the normalised moments to be expected from a scatterer modelled as a finite random walk with Poisson step number fluctuations [26]. Since the theoretical points still lie above the data it appears that the scatterers exhibit a degree of antibunching. Actual infrared Vidicon pictures of the scattered intensity corresponding to the two positions on the contrast curve mentioned above are shown in fig 14. The non-gaussian character of the pattern near the contrast peak is readily apparent.

Measurements have also been made of the second order (intensity) spatial coherence function of the scattered radiation against transverse displacements (Δ) of the detector. This quantity is defined by

$$g^{(2)}(\Delta) = \frac{\langle I(\underline{R}) I(\underline{R}+\underline{\Delta}) \rangle}{\langle I(\underline{R}) \rangle \langle I(\underline{R}+\underline{\Delta}) \rangle} \qquad (7)$$

where the averages are over different positions $\underline{R}$ of the detector. Measurements were restricted to detector positions around the $\theta = 0$ scattering direction, with detector displacements $\underline{\Delta}$ perpendicular to the axis of the system. A typical result is given in fig 15, which shows plots of $g^{(2)}(\underline{\Delta})$ for two different positions on the contrast curve, corresponding to gaussian and non-gaussian scattering. Two length scales may be identified in the decay of $g^{(2)}(\underline{\Delta})$. The shorter length ℓ_s is the speckle or interference scale; the relevant scatterer feature responsible is the total target width that illuminates the detector. The second scale length ℓ_D represents diffraction by the individual elements δ of the particle model over which the distortion of the incident wavefront varies by $\sim \lambda$; here the controlling aperture dimension is the element size δ. For the measurements reported here the diffraction scale length is of order 10^2 the interference length. This emphasises the fact that the intensity fluctuations are correlated over much longer distances than would be expected from conventional gaussian

scattering theory; an important factor when considering spatial diversity techniques.

The studies described above have made use of scattering surfaces produced by relatively uncontrolled means ie they have a complex fractal nature. A rather different approach is described in Hollins and Jordan [27]. In this, ion-beam milling techniques were used to produce a predetermined two-height pseudo-random phase-screen of rectangular grooves from which measurements of scattered CO_2 laser radiation were made. The surface height auto-correlation function resembled an exponentially decaying sinusoid and possessed characteristics that might make it suitable as a possible simplified model of other structures displaying short-range order and long-range disorder such as the near-periodic distributions of molecules in a liquid crystal or waves on a sea-surface. It is expected that the study of scatterers conforming to a pre-determined, analytically treatable pattern will be continued at Imperial College.

All of the surface structure measurements we have performed on solid surfaces have shown that they can be modelled by a fractal surface. Results from high resolution microwave radar returns from the sea have been analysed by Jakeman and Pusey [5] and more recently by K D Ward [29] who showed that under many conditions the scattered radiation follows a K-distribution. As seen from fig 13, this is not characteristic of a fractal scatterer. Jakeman [22] however has shown analytically that scattering from a sub-fractal (Type III surface) with a dimension D = 1.5 leads to K-distributed intensity fluctuations. The internationally agreed ocean wave power spectrum (Bretschneider formulation) also follows an approximate k^{-4} dependence, characteristic of a sub-fractal. It thus appears plausible that a sub-fractal may be a realistic model for the evaluation of sea scattering. To test this hypothesis we have carried out some preliminary experiments. Waves were generated in a small glass tank (350 x 220 mm) and photographed through the side. The waveheight verses distance along the tank was then measured from these photographs and the surface spatial power spectrum computed.

For D = 1.5, the surface height power spectrum of a sub-fractal should follow a power law

$$P_h(k) = \frac{C}{|\bar{k}|^4} \qquad (8)$$

As a sub-fractal is an integrated fractal, the surface profile of a sub-fractal should be relatively smooth. Fig 16(a) shows the integrated version of the fractal shown in Fig 6, the profile being integrated about its mean value. The relatively smooth shape, which one would expect from waves on a liquid is readily apparent; its power spectrum, which is shown in arbitrary units in Fig 16(b) has the expected gradient.

The preliminary laboratory experiments were extremely limited in dynamic range; to study phenomena which decay as k^{-4} requires large waves and high resolution. The waves produced in the tank were of height 10-20 mm and the resolution was of order 0.2 mm. A typical power spectrum is shown in fig 17. It is encouraging that it does indeed show a k^{-4} dependence over a limited range; it flattens off at higher spatial frequencies because of measurement limitations. Preparations are in progress to obtain more convincing data by

carrying out surface structure measurements over a wide range of sea states to be simulated in a 200 ft wave tank at AMTE (Gosport).

CONCLUSIONS

In this memo we have briefly outlined some of the current knowledge on non-gaussian scattering from rough surfaces. The effects can be generated without difficulty by using sufficiently small illuminated regions or by viewing the scattered radiation in the Fresnel region. We have shown that three principal surface types can be distinguished:

(1) Single-scale surfaces (Type II),

(2) multiple-scale surfaces ie fractal (Type I) and

(3) Sub-fractal surfaces (Type III).

We have shown that solid surfaces always appear to exhibit a fractal behaviour over a significant range of scale sizes; the existence of scale sizes smaller than the probing radiation wavelength gives rise to significant large angle scattering. On the other hand, the tentative evidence so far available suggests that liquid surfaces exhibit a sub-fractal behaviour.

Although the scattering measurements described in this memo have been carried out in the infra-red the results are probably viable for the whole of the electromagnetic spectrum, from visible scattering to microwave and radio scattering. No matter what the probing wavelength, in general scale sizes exist which span the region from somewhat less than to somewhat greater than it. The applications of scattering work are useful not only in perhaps allowing techniques to be developed for remote sensing of surface finish (eg crystal growing), but in explaining deviations from noise-like statistics in radar returns. For example, for large illuminated patch sizes and high grazing angles ($> 10^{o}$) it is found that, as expected, sea clutter obeys the central limit theorem and has Rayleigh distributed amplitude statistics [28]. When however the grazing angle is reduced and/or the radar resolution increased, this description no longer applies and the clutter is described as 'spiky'. These deviations from noise-like statistics have a considerable impact on performance, and work on characterising them in terms of scattering models would be of benefit.

Much work still remains to be carried out on scattering, both from solid and liquid surfaces. In particular, the effect of grazing angle scattering from fractal surfaces, more studies of the effect of structure smaller than the probing wavelength and modelling of realistic sea surfaces. It should also be noted that similar power law formulations are applicable to propogation through atmospheric turbulence. It is therefore to be expected that a similar mixture of theory and laboratory experiments (using visible and infra-red lasers) to those described here for scattering would give considerable insight into the understanding and modelling of atmospheric turbulence. Finally it should be mentioned that the subject of fractal structures is of interest in its own right, and may possibly provide new ideas in microchip design, allowing efficient communication between all parts of a very large and complex device.

REFERENCES

[1] Dainty, J. C., Ed, Laser Speckle and Related Phenomena, Plenum (1975)

[2] Jakeman, E., In Applications of Speckle Phenomena, ed. W. H. Carter, SPIE Proc. 243 (Society of Photo-optical Instrumentation Engineers, Bellingham 1980) p9

[3] Jakeman, E., Parry, G., Pike, E. R., and Pusey, P. N., Contemp. Phys. 19, 127 (1978)

[4] Upstill, C., Proc. Roy. Soc. A365, 95 (1979)

[5] Jakeman, E., Pusey, P. N., IEEE Trans. Antennas and Propagation, AP-24, No 6, 806 (1976)

[6] Zardecki, A., In Inverse Source Problems in Optics, ed., H. P. Baltes, Topics Current Phys 9 (Springer, Berlin, Heidelberg, New York 1978) p.155

[7] Berry, M. V., J. Phys A, 10, 2061 (1977)

[8] Berry, M. V., Adv. Phys., 25, 1 (1976)

[9] Jakeman, E., Pusey, P. N., RRE Memo 2874 (1974)

[10] Jakeman, E., RSRE Memo 3255 (1980)

[11] Pusey, P. N., Jakeman, E., J. Phys A, 8, 392 (1975)

[12] Ohtsubo, J., Asakura, T., Opt. Comm. 25, 315 (1978)

[13] Chandley, P. J., Escamilla, H. M., Opt. Comm. 29, 151 (1979)

[14] Mandelbrot, B. B., Fractals (Freeman, San Francisco 1977)

[15] Jakeman, E. In RSRE Newsletter and Research Review, No 6, 16 (1982)

[16] Jakeman, E., McWhirter, J., J. Phys A. 10, 1599 (1977)

[17] Rumsey, V. H., Radio Sci., 10, 107 (1975)

[18] Berry, M. V., J. Phys A. 12, 781 (1979)

[19] Marians, M., Radio Sci. 10, 115 (1975)

[20] Furuhama, Y., Radio Sci. 10, 1037 (1975)

[21] Jordan, D. L., Hollins, R. C., Jakeman, E., Appl. Phys. B, 31, 179 (1983)

[22] Jakeman, E., J. Opt. Soc. Am., 72, No 8, 1034 (1982)

[23] Jordan, D. L., Hollins, R. C., Opt. Acta 13, 417 (1983)

[24] Sayles, R. S., Thomas, T. R., Nature, 271, 431 (1978)

[25] Jordan, D. L., Hollins, R. C., Jakeman, E., Opt. Comm., 49, No 1, 1 (1984)

[26] Pusey, P. N., In Photon Correlation Spectroscopy and Velocimetry, Eds. H. Z. Cummins and E. R. Pike (Plenum, New York 1977)

[27] Hollins, R. C., Jordan, D. L., Opt. Acta, 30, No 12, 1725 (1983)

[28] Ward, K. D. Radar 82

[29] Ward. IEEE

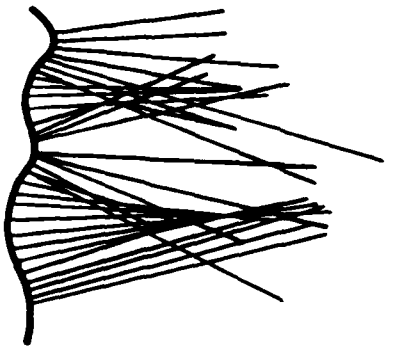

FIG. 1(a)

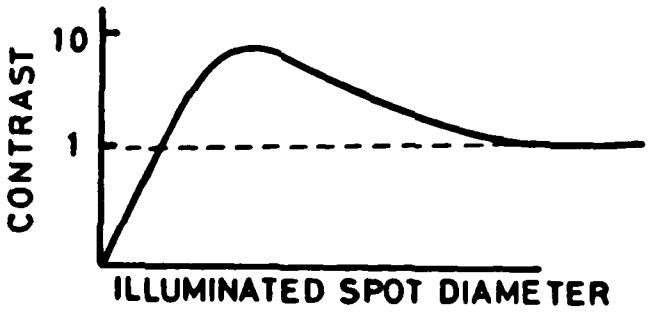

FIG. 1(b)

Fig 1(a) Smoothly varying surface producing focussing and caustics (singularities)

Fig 1(b) Contrast verses illuminated spot diameter

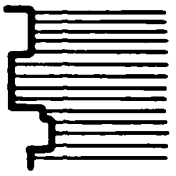

FIG. 2

Fig 2 A stepped surface generating no ray density fluctuations

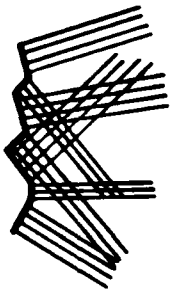

FIG. 3

Fig 3 A surface of randomly oriented facets generates elementary ray density fluctuations but no singularities

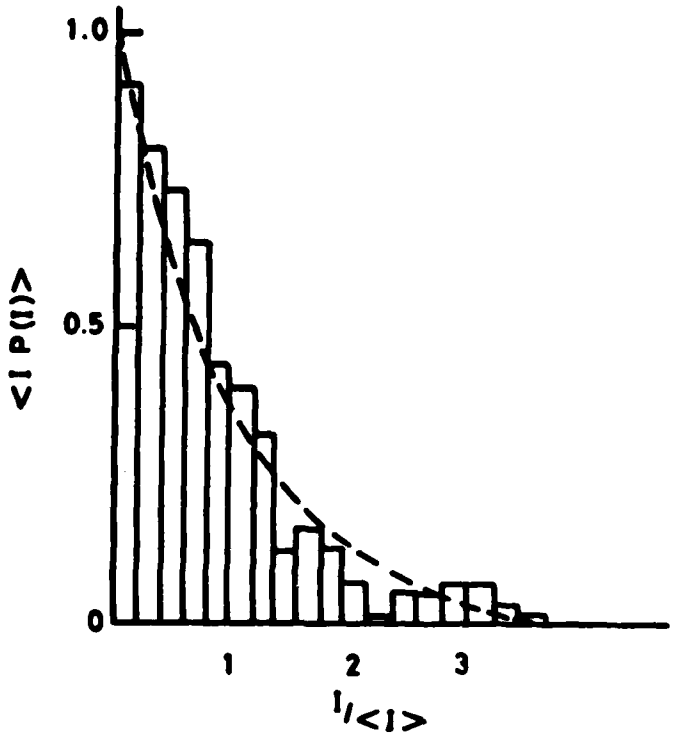

Fig 4 Direct detection normalised probability density function. The broken line represents a negative exponential distribution

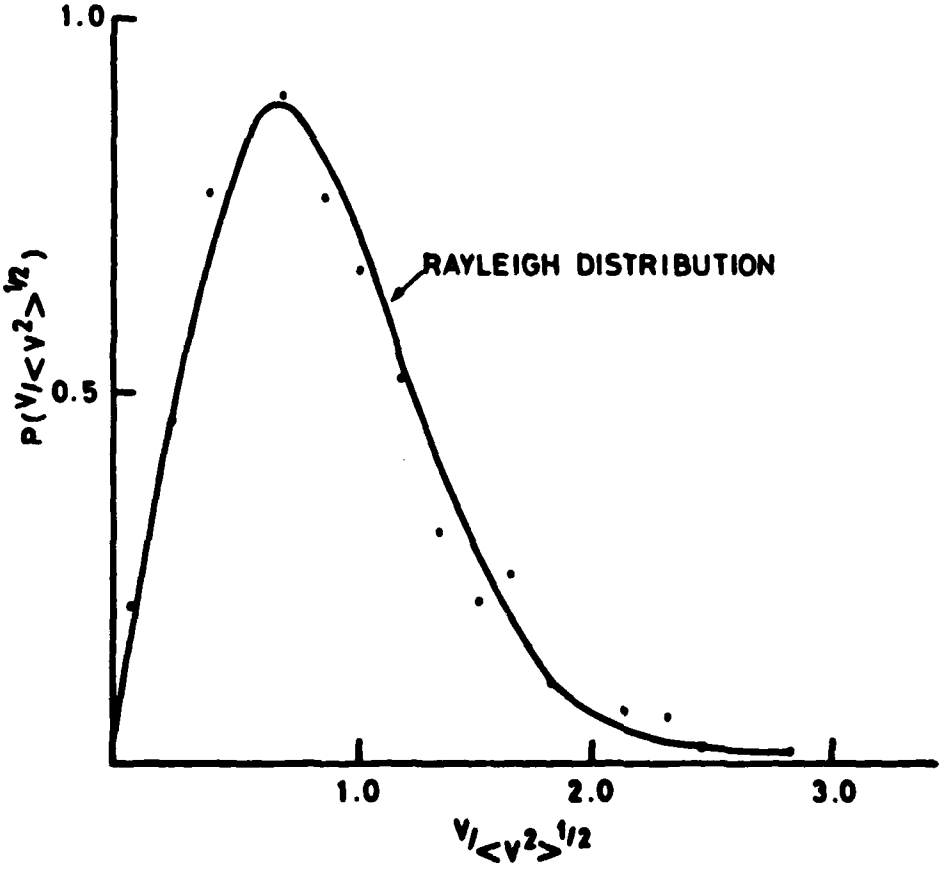

Fig 5 Measured (points) and theoretical (curve) first order probability density function for heterodyne detection

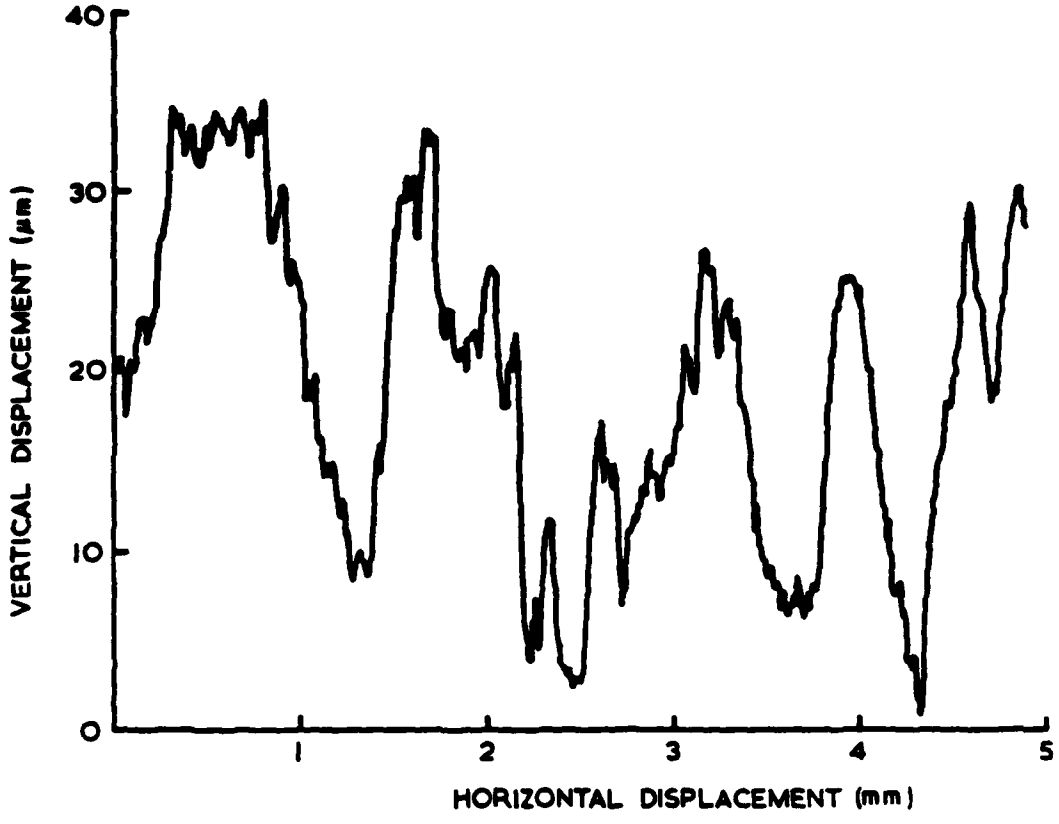

Fig 6 Surface height profile of the germanium target

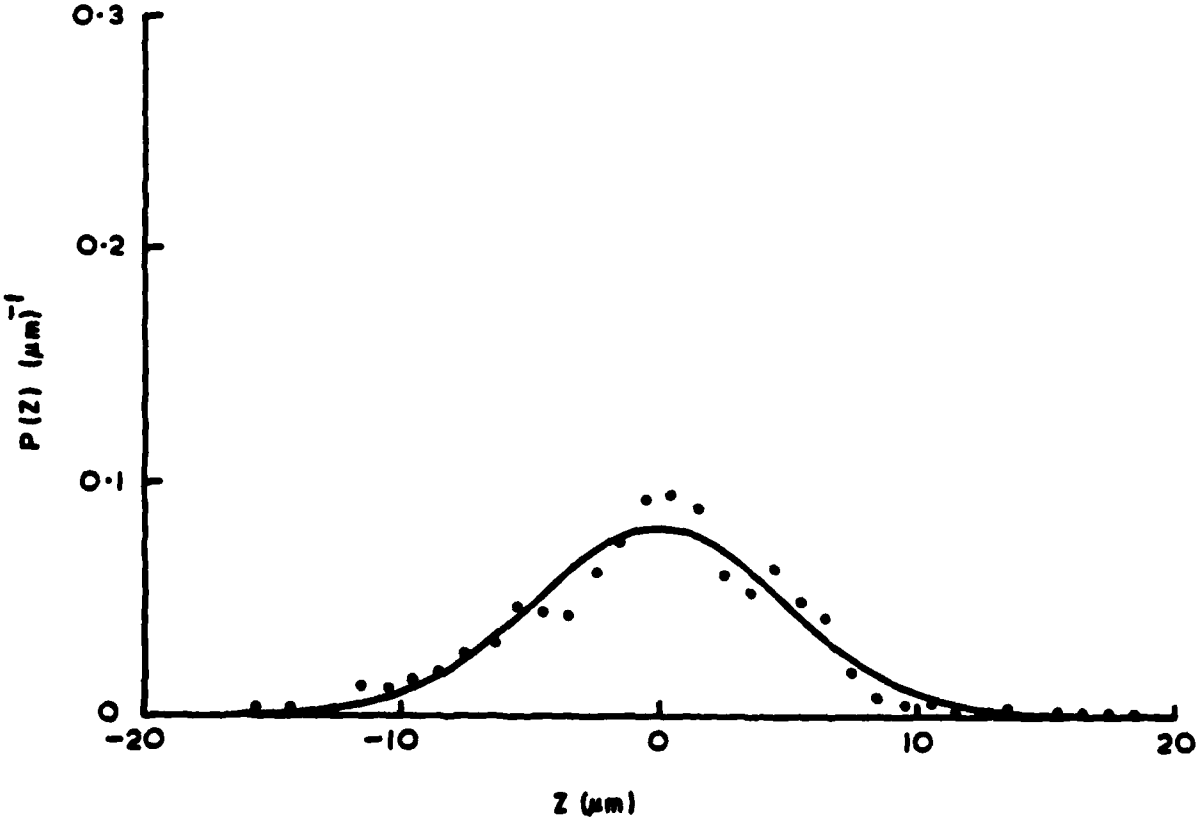

Fig 7 Probability density distribution for the height difference Z [=h(x+δ) - h(x)] between two points of separation δ=70 μm

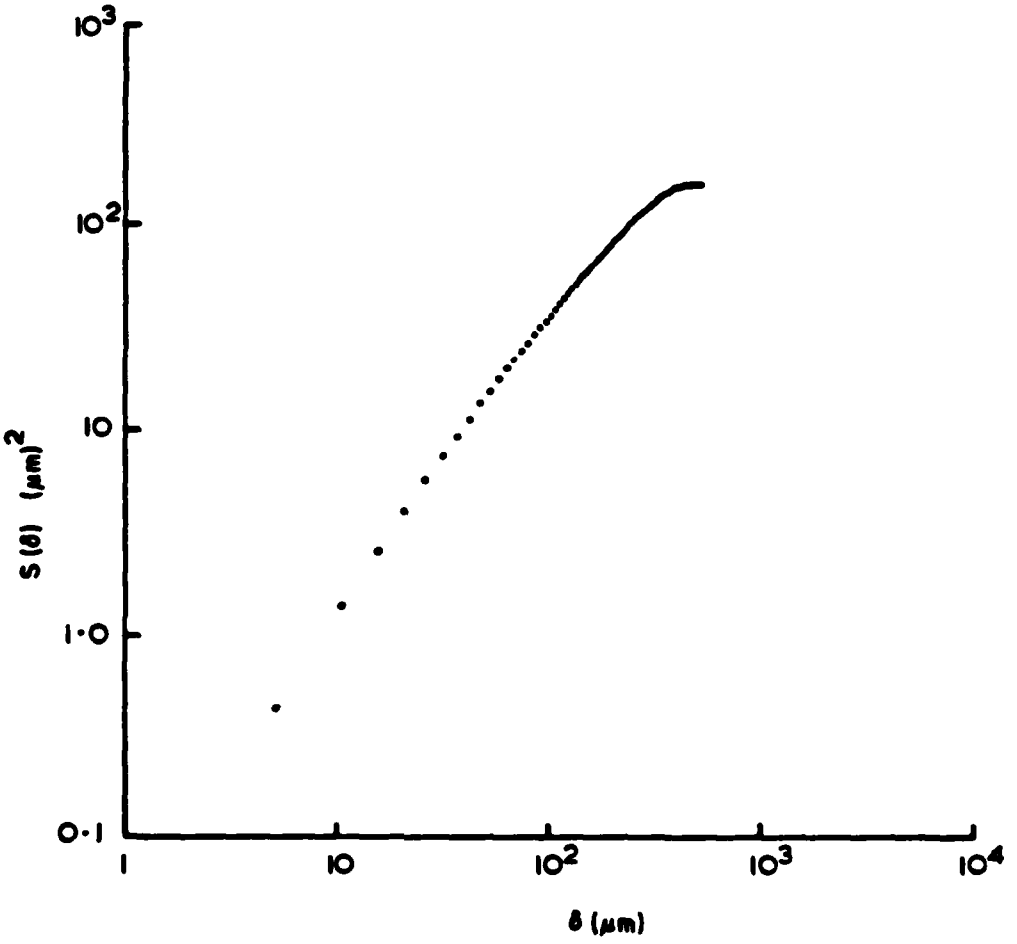

Fig 8 Structure function of germanium surface

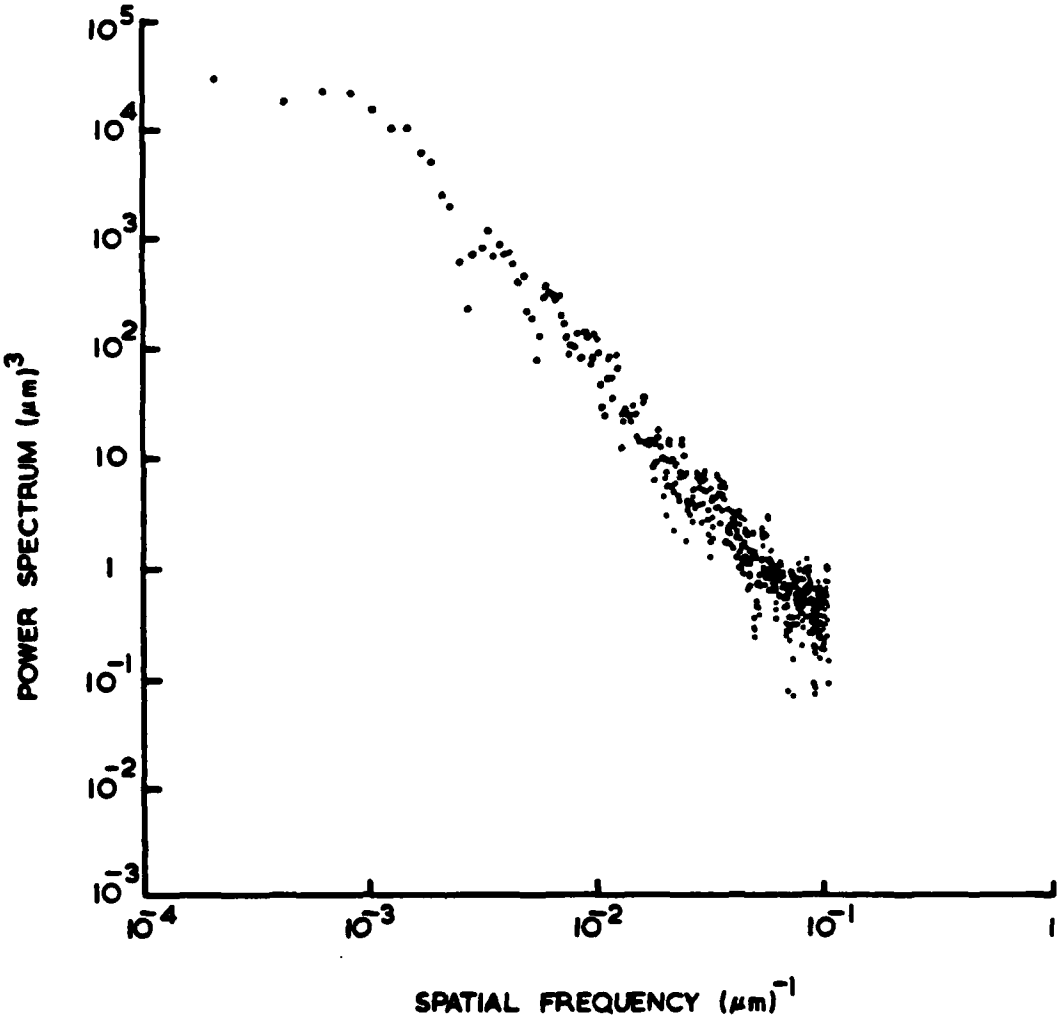

Fig 9 Spatial power spectrum of the surface profile

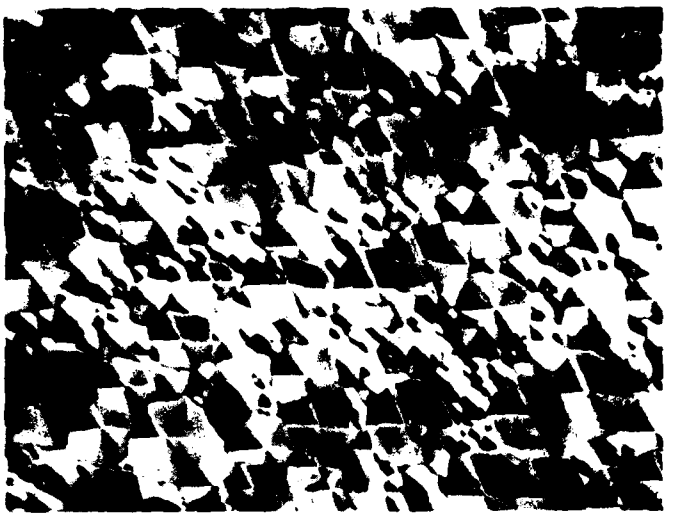

Fig 10 Photomicrograph of MOCVD grown GaAs (12 mm on picture ≡ 50 μm)

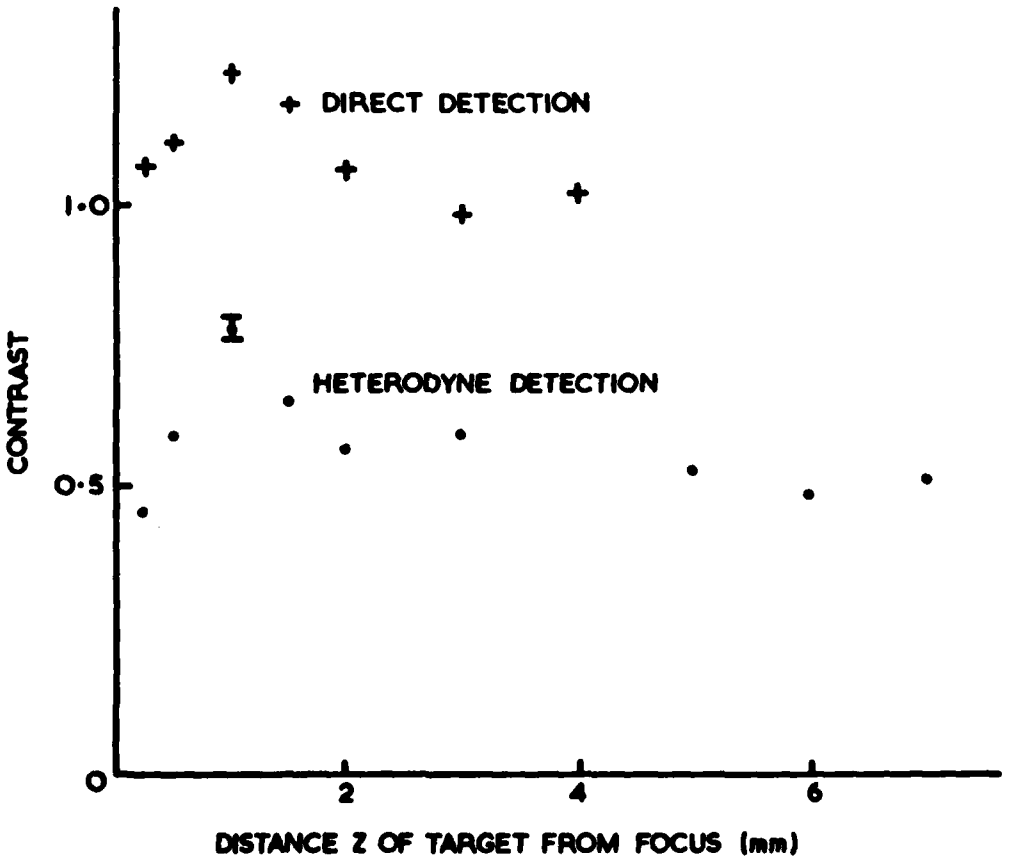

Fig 11 Contrast in the Fresnel region as a function of distance from focal plane of lens

• EXPERIMENT

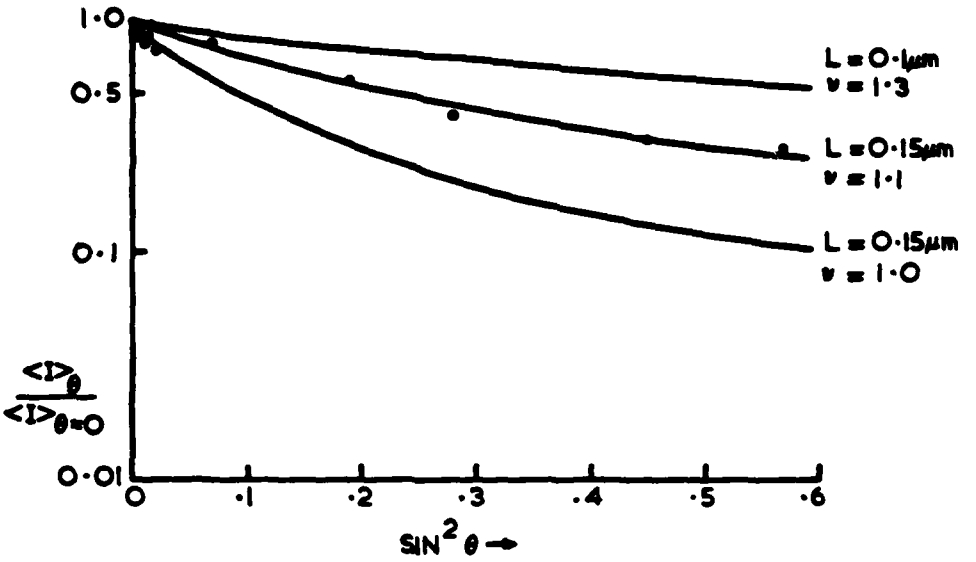

Fig 12 Angular dependence of the mean scattered intensity

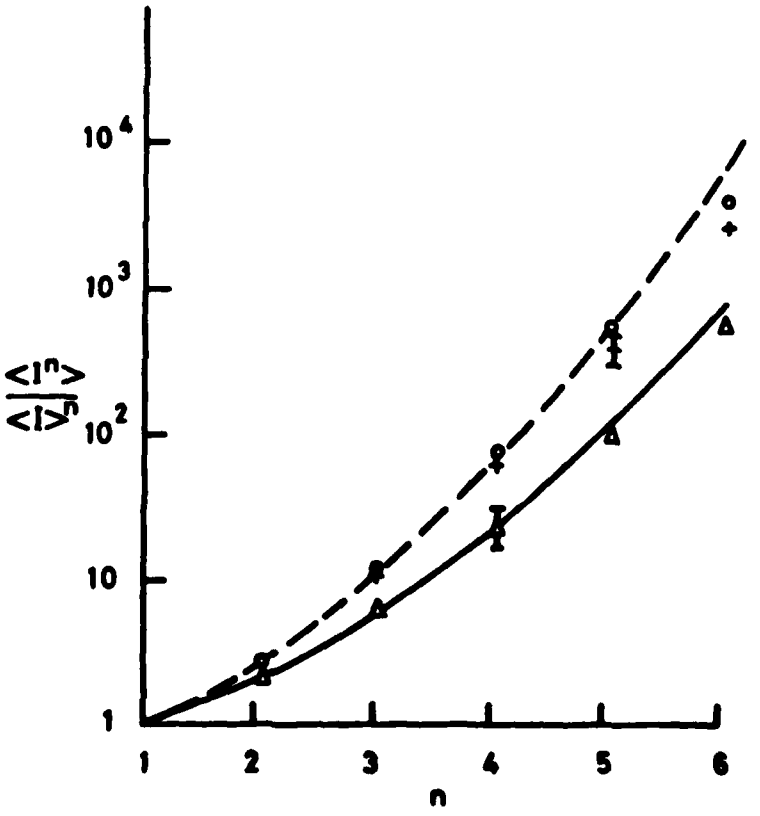

Fig 13 Normalised moments of the scattered intensity distribution:

Δ measured values well away from contrast peak
\+ measured values near contrast peak
Solid line: negative exponential distribution
Broken line: K distribution
O: Number fluctuation model

(a)

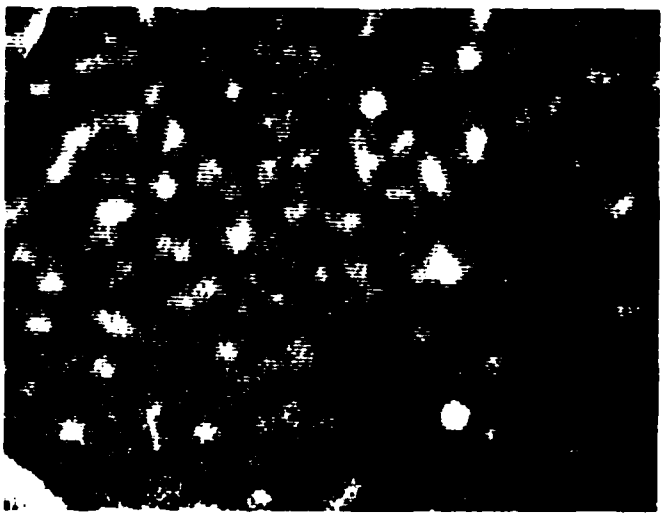

(b)

Fig 14 Vidicon pictures of scattered radiation:

(a) Near contrast peak

(b) Well away from contrast peak

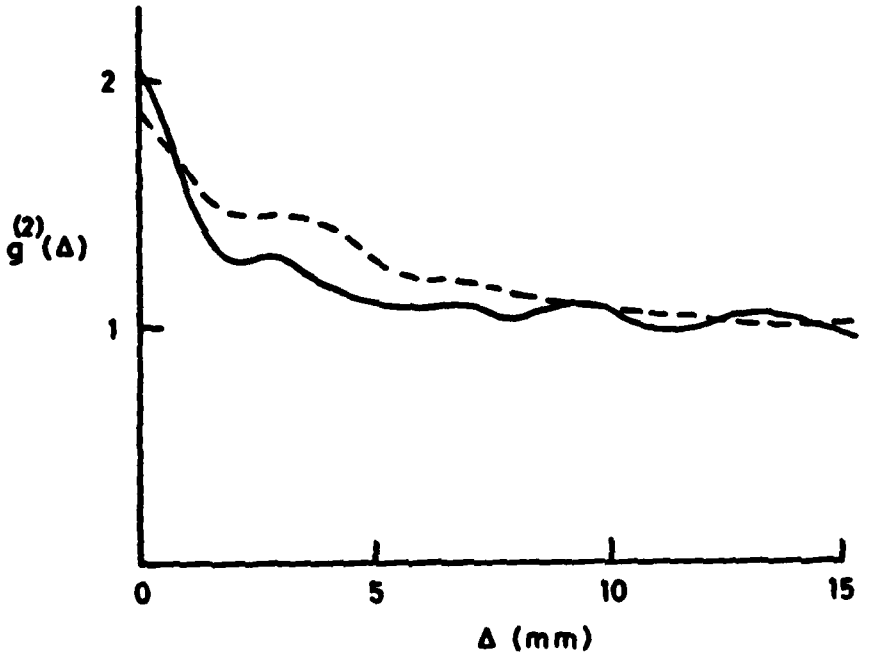

Fig 15 Transverse spatial coherence function:

Solid line: Well away from contrast peak
Broken line: Near contrast peak

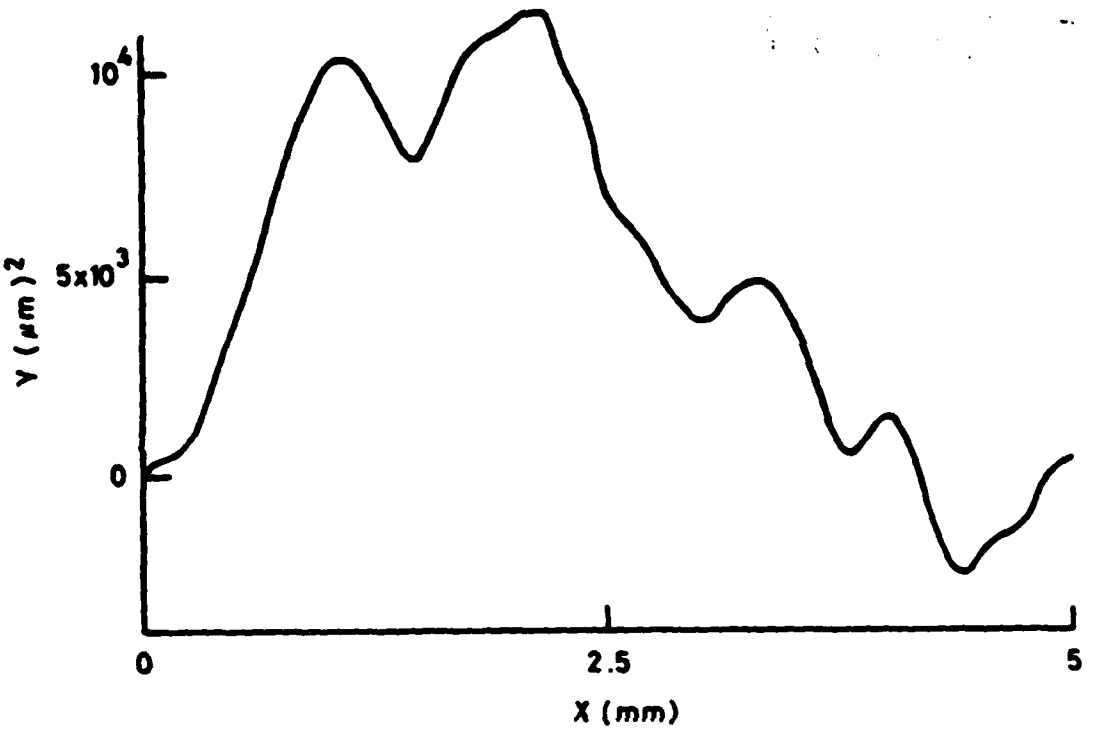

(a)

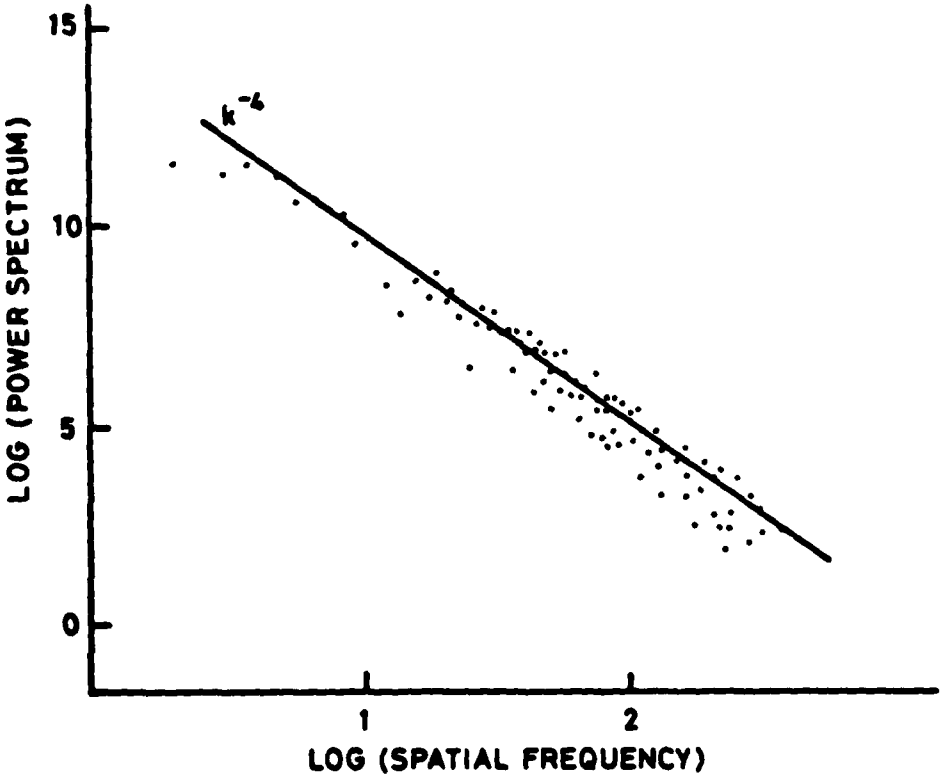

(b)

Fig 16(a) Integrated fractal surface profile

Fig 16(b) Power spectrum of Integrated fractal. The line has a slope of -4

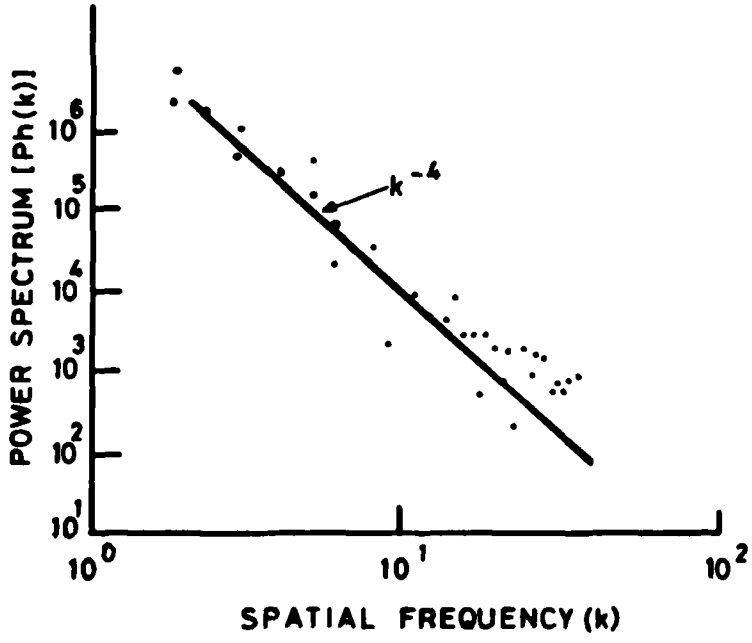

Fig 17 Power spectrum (arb-units) of water waves. Solid line has a k^{-4} slope for reference

D

E

D

B4